

INFLUENCE OF UPSTREAM TURBULENCE ON SELF-SUSTAINED OSCILLATIONS IN AN OPEN CAVITY

Sang Bong Lee

Department of Mechanical Engineering,
Korea Advanced Institute of Science and Technology
373-1, Guseong-dong, Yuseong-gu, Daejeon, 305-701 Korea
sblee1977@kaist.ac.kr

Hyung Jin Sung

Department of Mechanical Engineering,
Korea Advanced Institute of Science and Technology
373-1, Guseong-dong, Yuseong-gu, Daejeon, 305-701 Korea
hjsung@kaist.ac.kr

ABSTRACT

Direct numerical and large eddy simulations of incompressible turbulent flows over deep and shallow cavities were performed in the range of $600 \leq Re_D \leq 12000$ to investigate the influence of the incoming turbulent boundary layer on self-sustained oscillations of the shear layer. When the turbulent boundary layer of $Re_\theta = 300$ approached the open cavity with $Re_D = 3000$, the energy spectra of the pressure fluctuations showed energetic frequencies in the range of $0.15 \leq \omega_\theta \leq 0.3$. Conditionally averaged flow fields disclosed that the energetic frequencies arise from the separation of high speed streaky structures rather than from a geometric peculiarity of the cavity. The same energetic frequencies were observed in a backward-facing step flow as well as in deep and shallow cavity flows, despite the different geometries of these systems. In the turbulent cavity flow of $Re_D = 12000$, however, the peak frequencies of the energy spectra at cavity lengths of $L/D = 1$ and 2 were found to correspond to the N th modes with $N = 2$ and 3 respectively. These N th modes were very similar to the frequency characteristics of self-sustained oscillations reported for laminar cavity flows. Inspection of instantaneous pressure fluctuations as well as spanwise-averaged pressure fluctuations revealed that regular shedding of quasi two-dimensional vortical structures was responsible for the peak frequency in the energy spectra.

INTRODUCTION

Flows over open cavities occur in many engineering applications, for example landing gear wells and bomb bays in aircraft and sunroofs in automobiles. The presence of the open cavity generates strong self-sustained oscillations of velocity, pressure and, occasionally, density. To understand the mechanism underlying such oscillations and prevent undesirable effects, numerous experimental and numerical studies have been carried out since Norton (1952) investigated the buffeting of bomber airplanes due to air flow over their bomb bays. Nevertheless it is unclear whether the turbulent incoming boundary layer can give rise to self-sustained oscillations in incompressible turbulent

cavity flows (Rockwell 1998). Pereira & Sousa (1994, 1995) observed periodically oscillating shear layers in the flow of a turbulent incoming boundary layer over an open cavity. Lin & Rockwell (2001) also observed self-sustained oscillations in water-tunnel experiments, and suggested that the oscillations are related to large-scale vortical structures. In contrast, Grace, Dewar & Wroblewski (2004) found no evidence of self-sustained oscillations in velocity and pressure data from their experiment with a turbulent incoming boundary layer. Chatellier, Laumonier & Gervais (2004) observed self-sustained oscillations of the mixing layer in their experiments, and theoretically analyzed the fluctuating behaviors of turbulent cavity flows at low Mach number. They suggested that the oscillating process is not governed by periodic shedding of coherent structures but by convective waves of naturally unstable mixing layer. However, Ashcroft & Zhang (2005) observed the shedding of large-scale vortical structures by Galilean decomposition of the instantaneous and fluctuating velocity fields. The coherent vortical structures were present in the majority of PIV images, although well-defined structures were not always observed. The authors pointed out small peaks in the pressure spectra as evidence of weak tonal components; however strong self-sustained oscillations were not observed. The main objective of the present study was to elucidate whether a fully turbulent boundary layer can give rise to self-sustained oscillations and, if such oscillations exist, whether they are related to coherent vortex formation. To achieve this, we performed DNSs and LESs of incompressible turbulent flows over deep and shallow cavities for a wide range of Reynolds number ($600 \leq Re_D \leq 12000$), where Re_D is the Reynolds number based on the cavity depth. The present simulations used L/θ values of up to 80, which is sufficiently large to identify the existence of self-sustained oscillations. The turbulent flow over a backward-facing step was also simulated for comparison. Turbulence statistics and frequency spectra of fluctuating quantities were obtained to analyze the fluctuating behaviors of the turbulent cavity flows. Conditional-averaging and spanwise-averaging were employed to extract spatial maps of the pressure fluctuations.

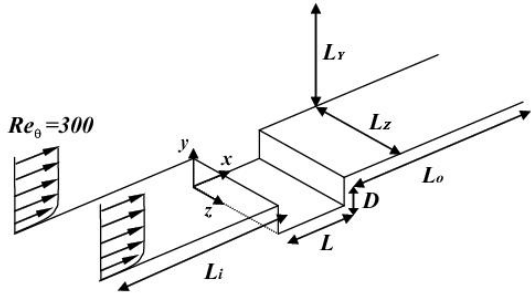


Figure 1: Schematic diagram of computational domain.

NUMERICAL METHOD

A schematic diagram of the computational domain is shown in Figure 1. For all of the present simulations, the turbulent boundary layer was provided at the inlet with the realistic velocity fluctuations of $Re_\theta = 300$. DNSs of incompressible flows over an open cavity were performed for two Reynolds numbers, $Re_D = 600$ and 3000 . The cavity flows at high Reynolds number ($Re_D = 12000$) were simulated using a LES with a dynamic sub-grid scale model. The simulation conditions used in the present study are summarized in Table 1.

Table 1: Simulation conditions.

Re_D	L/D , L/θ	$N_x \times N_y \times N_z$
600	1, 2	289×95×129
	2, 4	321×95×129
3000	1, 10	417×133×129
	2, 20	513×133×129
	4, 40	705×133×129
	6, 60	897×133×129
	∞ , ∞	577×133×129
12000	1, 40	705×169×257
	2, 80	897×169×257

IDENTIFICATION OF PRESSURE FLUCTUATIONS

Before examining in detail whether self-sustained oscillations exist, it is helpful to compare the characteristics of the pressure fluctuations observed in the turbulent cavity flows at the three Reynolds numbers. Figure 2 shows the energy spectra of the pressure fluctuations at $(x/D, y/D) = (0.5, 1.0)$ for length-to-depth ratios (L/D) of 1 and 2. The energy spectra of the systems with $Re_D = 600$, 3000 and 12000 are shown in Figures 2(a), (b) and (c), respectively. The frequency is non-dimensionalized by using the momentum thickness of the incoming turbulent boundary layer, i.e. $\omega_\theta = 2\pi f \theta / U_\infty$. Energetic frequencies are observed in all of the spectra, although the pressure fluctuations at $Re_D = 600$ show broad spectra due to small energetic increases. As shown in Figures 2(a) and (b), the pressure fluctuations are energetic in the frequency range of $0.15 \leq \omega_\theta \leq 0.3$, regardless of the length-to-depth ratio. This suggests that the energetic pressure fluctuations observed for the $Re_D = 600$ and 3000 systems are little affected by the

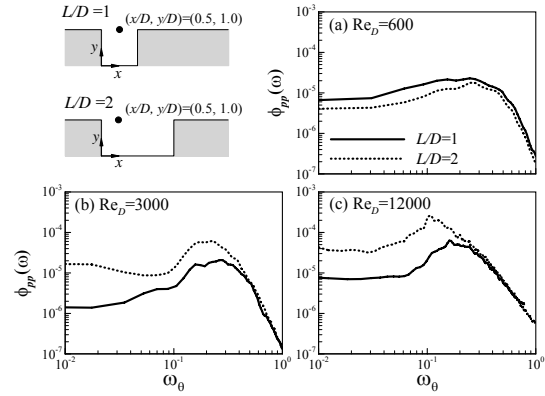


Figure 2: Energy spectra of pressure fluctuations measured at $(x/D, y/D) = (0.5, 1.0)$.

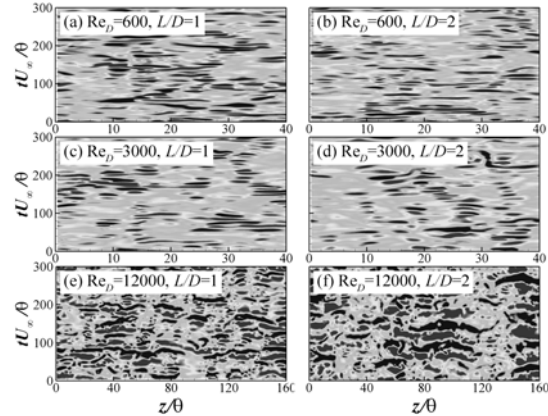


Figure 3: Time histories of pressure fluctuations corresponding to the energy spectra of Figure 2. Spanwise length and time are normalized by the momentum thickness of incoming turbulent boundary layer.

geometrical dimensions of the cavity. In the $Re_D = 12000$ spectra (Figure 2(c)), however, the peak in the fluctuation spectrum shifts to lower frequency as the cavity length increases. Specifically, the frequency range exhibiting energetic pressure fluctuations is $0.15 \leq \omega_\theta \leq 0.2$ for $L/D = 1$, but about 0.08 to 0.12 for $L/D = 2$. This frequency shift in the fluctuation spectrum as a function of cavity length is very similar to the previous observation that, as the cavity length was increased, the frequency of self-sustained oscillations in a system with a laminar incoming boundary layer decreased (Gharib & Roshko 1987).

In order to characterize the pressure fluctuations in the frequency range around the peak in the energy spectrum, a more instructive view can be derived by examining the evolution over time of the fluctuation distribution in the spanwise direction. Figure 3 shows such time histories, in which the horizontal and vertical axes represent the spanwise direction and time, respectively, and the pressure fluctuations corresponding to the energy spectra of Figure 2 are represented. Close inspection of Figure 3 discloses that the pressure fluctuations in the $Re_D = 600$ and 3000

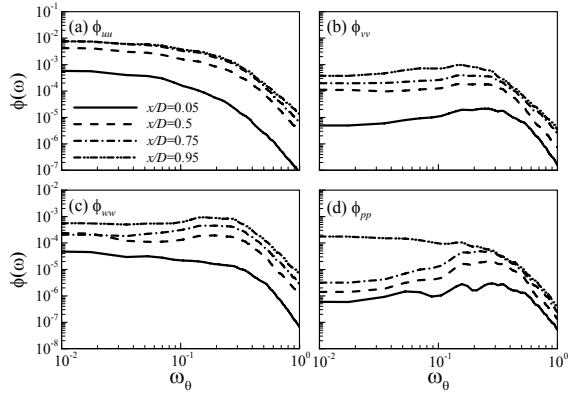


Figure 4: Energy spectra of fluctuating quantities at four streamwise locations between the leading edge ($x/D = 0$) and the trailing edge ($x/D = 1$). The length-to-depth ratio is unity and $Re_D = 12000$.

systems (Figures 3(a)–(d)) exhibit qualitatively different characteristics from those in the $Re_D = 12000$ system (Figures 3(e) and (f)). Specifically, at $Re_D = 600$ and 3000 , the pressure undergoes three-dimensional fluctuations intermittently. At $Re_D = 12000$, by contrast, quasi two-dimensional pressure fluctuations are regularly observed, albeit with slight variations away from two-dimensional behavior. Note that the spanwise length scale of Figures 3(e) and (f) is four times longer than that of Figures 3(a)–(d). Detailed comparison of the $Re_D = 12000$ systems with $L/D = 1$ and $L/D = 2$ (Figures 3(e) and (f) respectively) indicates that the time scale of the pressure fluctuations increases with increasing cavity length. This finding is consistent with the dependence of energetic frequencies on cavity length shown in the energy spectra of the $Re_D = 12000$ system.

SPECTRAL CHARACTERISTICS AT $Re_D = 3000$

To examine the spectral characteristics at a length-to-depth ratio of unity and $Re_D = 3000$, we determined the frequency spectra of the velocity and pressure fluctuations at four representative streamwise locations between the leading edge ($x/D = 0$) and the trailing edge ($x/D = 1$): the region immediately downstream of the leading edge ($x/D = 0.05$), the center of the cavity ($x/D = 0.5$ and 0.75), and the impingement region near the trailing edge ($x/D = 0.95$). For a length-to-depth ratio of unity, no energetic frequencies are observed in the spectra of streamwise velocity fluctuations (Figure 4(a)). The spectra of the vertical and spanwise velocity fluctuations show energetic frequencies, although the energetic increases are very small (Figure 4(b) and (c)). In the spectra of the pressure fluctuations, however, energetic frequencies are clearly observed between $\omega_\theta = 0.15$ and 0.3 (Figure 4(d)). This energetic frequency range is converted to $0.24 \leq St_D \leq 0.5$ using $St_D = fD/U_\infty$, which is consistent with the previous observation of slightly more intense pressure fluctuations at the frequencies of $St_D = 0.38$ and 0.51 (Chang et al. 2006). Why are energetic frequencies observed in the frequency spectra of pressure fluctuations? To answer the question, we examined in detail the time

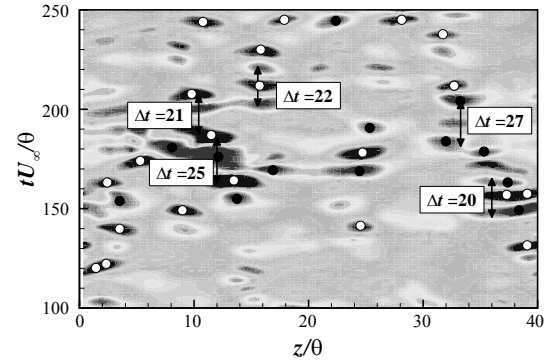


Figure 5: Time histories of pressure fluctuations measured at $(x/D, y/D) = (0.5, 1.0)$ when the length-to-depth ratio is unity. The white and black circles represent local minimum points satisfying $p < -1.5p_{rms}$ and local maximum points satisfying $p > 1.5p_{rms}$, respectively.

evolution of the pressure fluctuations at $(x/D, y/D) = (0.5, 1.0)$ at locations along the spanwise direction, as shown in Figure 5. Figure 5 shows parts of Figure 3(c) where the horizontal and vertical axes represent the spanwise direction and time, respectively. Both time and spanwise length are non-dimensionalized by using the momentum thickness of the incoming turbulent boundary layer. As discussed, the pressures show intermittent three-dimensional fluctuations with periods between 20 and 30. The range of the periods is in accord with the energetic frequencies of the pressure spectra ($0.15 \leq \omega_\theta \leq 0.3$). This indicates that the intermittent strong fluctuations in the pressure are responsible for the energetic frequencies.

To show the coherent structures that generate the intermittent pressure fluctuations, the instantaneous flows were conditionally averaged. By analyzing the full time histories of the pressure fluctuations at $(x/D, y/D) = (0.5, 1.0)$, we identified the points on the map of time versus spanwise location where the pressure fluctuations were a local minimum satisfying $p < -1.5p_{rms}$ or a local maximum satisfying $p > 1.5p_{rms}$. For example, in Figure 5, the white and black circles represent the local minima and maxima identified in this way, respectively. At each time point, the instantaneous flow was averaged around the spanwise locations. Figure 6(a) shows contour plots of the pressure fluctuations and vector plots of the velocity fluctuations in the lip plane under the conditions of local minimum and $p < -1.5p_{rms}$ while Figure 6(b) displays two-dimensional plots on the cut-off plane of Figure 6(a). The dotted lines represent negative pressure fluctuations whereas the solid lines represent positive pressure fluctuations. As seen in Figures 6(a) and (b), the counter-clockwise rotating vectors represent a vortical structure with strong negative pressure fluctuations. This structure has length scales of $\Delta x/D = 0.4 \sim 0.5$ in the streamwise direction and $\Delta z/D \leq 1$ in the spanwise direction. Figure 6(c) shows three-dimensional pressure fluctuations averaged under the condition of local maximum and $p > 1.5p_{rms}$, while Figure 6(d) displays two-dimensional plots on the cut-off plane of Figure 6(c). These representations show that positive pressure fluctuations

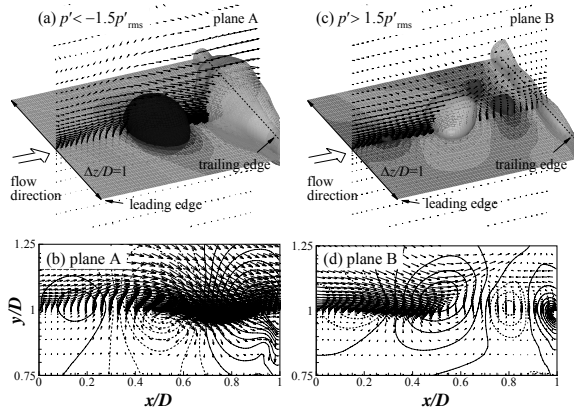


Figure 6: Conditional-averaged contours of pressure fluctuations and vectors of velocity fluctuations.

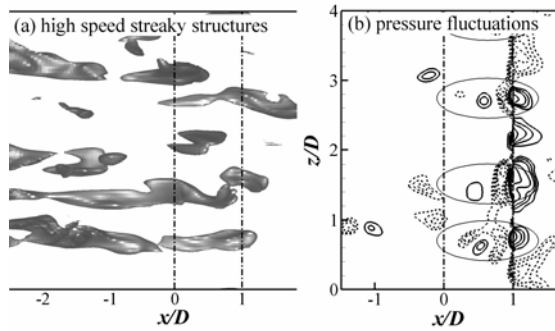


Figure 7: Top-view of instantaneous high speed streaky structures and pressure fluctuations on the plane of $y/D=1$. The high speed streaky structures are represented by the contours of $u' \geq 0.18U_\infty$.

occur between two vortical structures. The vortical structure near the leading edge has just been generated and the other vortical structure is likely to impinge on the trailing edge. The positive pressure fluctuations are interpreted as being induced by the two vortical structures, as observed in the vortical shedding of a separated shear layer. Moreover, the strong negative pressure fluctuations of the vortical structures and the induced positive pressure fluctuations are responsible for the intermittent pressure fluctuations.

As seen in Figures 6(a)–(d), the positive fluctuations of streamwise velocity ($u > 0$) occur near the leading edge and in the vicinity of the center along the lip line of the cavity geometry. It is interesting to note that the vertical distribution of u' is very similar to that of the incoming turbulent boundary layer. For example, the maximum fluctuations are observed near $y/D=1.07$ (Figures 6(b) and (d)), which exactly corresponds to $y^+ \approx 12$ of the turbulent boundary layer, where the streamwise velocity fluctuations are most intense. It is expected that the positive streamwise velocity fluctuations observed over the cavity represent high speed streaky structures of the incoming turbulent boundary layer. Considering that the Kelvin-Helmholtz instability arises when the velocity difference between shear layers

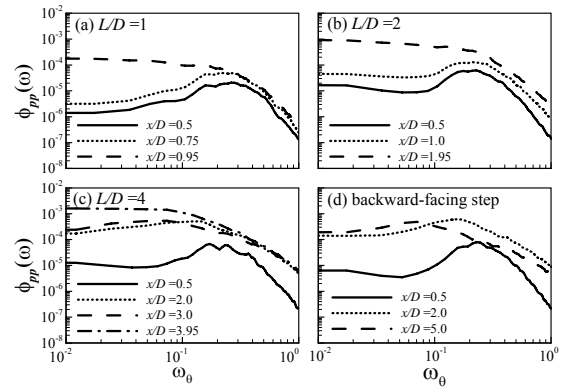


Figure 8: Frequency spectra of pressure fluctuations when the cavity length increases.

exceeds a certain level, it is natural that the high speed streaky structures can make the separated shear layer locally unstable due to the large velocity difference. Visualization of snapshots of the flow supports the notion that the high speed streaky structures of the incoming turbulent boundary layer play a significant role in the generation of the observed intermittent pressure fluctuations. Figure 7(a) displays a snapshot of the high speed streaky structures (represented by showing only contours with $u' \geq 0.18U_\infty$) in the plane $y/D=1$, while Fig. 7(b) shows a contour plot of the pressure fluctuations in the same plane. In Figure 7(b), the solid and dotted lines represent positive and negative pressure fluctuations, respectively. Comparison of Figures 7(a) and (b) shows a strong correlation between the high speed streaky structures and the regions of positive and negative pressure fluctuations, consistent with the high speed streaky structures passing over the cavity generating the energetic pressure fluctuations with three-dimensionality.

Figure 8 shows the frequency spectra of pressure fluctuations for systems with cavity lengths of $L/D=1, 2$ and 4 . The pressure fluctuations are obtained at several streamwise locations between the leading edge and the trailing edge along the lip line of the cavity geometry. Near the leading edge ($x/D=0.5$), all spectra show energetic frequencies in the range of $0.15 \leq \omega_0 \leq 0.3$ regardless of the length-to-depth ratio. In the center of the $L/D=1$ and 2 cavities (dotted lines of Figure 8(a) and (b) respectively), the energetic frequencies are observed in the same range ($0.15 \leq \omega_0 \leq 0.3$). In the center of the $L/D=4$ cavity (dotted or dashed lines of Figures 8(c)), however, the pressure fluctuations show energetic spectra at frequencies less than $\omega_0=0.15$. Considering that the large-scale vortical shedding of the flow over a backward-facing step takes place in the vicinity of $\omega_0=0.07$, as shown in Figure 8(d), large-scale vortical structures are likely to begin to form in the shallow $L/D=4$ cavity, but the trailing edge impedes further development of those structures. The disrupting influence of the trailing edge leads to considerable variation in the large-scale vortical structures, and well-defined large structures are not regularly observed.

SPECTRAL CHARACTERISTICS AT $Re_D=12000$

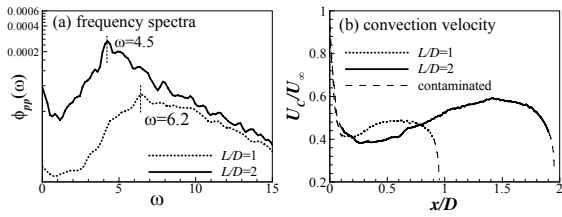


Figure 9: Frequency spectra and convection velocity of pressure fluctuations when $Re_D = 12000$. The convection velocity (U_C) is contaminated near the leading and trailing edges as indicated by dashed lines in (b).

As mentioned early, the pressure fluctuations in the $Re_D = 12000$ system correspond to the ‘high Reynolds number regime’, where quasi two-dimensional pressure fluctuations are regularly observed and the frequencies of energetic fluctuations decrease as the cavity length increases. Figure 9(a) shows the frequency spectra of pressure fluctuations in the $Re_D = 12000$ cavity flows with length-to-depth ratios of 1 and 2. Here the pressure fluctuations are measured at $(x/D, y/D) = (0.5, 1.0)$ and the frequency is non-dimensionalized using the cavity depth, i.e., $\omega_0 = 2\pi f D / U_c$. The peak frequency of energetic pressure fluctuations decreases from $\omega_{peak} = 6.2$ to 4.5 as the cavity length increases. This decrease in energetic frequency with increasing cavity length is very similar to the trend observed previously in the frequency of self-sustained oscillations in the flow over an open cavity with a laminar incoming boundary layer. Gharib & Roshko (1987) found that the oscillating frequency of ‘Mode II’ decreased from 6 Hz to 4 Hz as the length-to-depth ratio increased from 0.65 to 1.05, and that the shear layer oscillation shifted to ‘Mode III’ for ratios larger than 1.1. The oscillating frequencies of Modes II and III are determined by the relation

$$\frac{L}{\lambda_x} = \frac{fL}{U_c} = N \quad (1)$$

where λ_x is the streamwise wavelength of oscillation, f is the oscillating frequency, U_c is the convection velocity, and N is the number of wavelengths of fundamental frequency contained by the cavity length in the N th mode of oscillation.

To compare the dependence of energetic frequencies on cavity length with the frequency characteristics of self-sustained oscillations in laminar cavity flows, we calculated the local convection velocity (U_C) of pressure fluctuations from two-point time correlations (Figure 9(b)). Close examination of the time correlations indicates that the convection velocity is contaminated near the leading and trailing edges, as indicated by dashed lines of Figure 9(b). In calculating the streamwise averaged convection velocity (U_{Cavg}), which is needed to compare the peak frequency of Figure 9(a) with the oscillating frequency of laminar cavity flows, the regions with contaminated convection velocities were excluded. The streamwise averaged convection velocities are calculated as $U_{Cavg} = 0.475$ for $L/D = 1$ and $U_{Cavg} = 0.490$ for $L/D = 2$. By substituting the convection velocities into Equation (1), the peak frequencies of Figure 20(a) are expressed as $fL/U_{Cavg} = 2.08$ ($N = 2$) for $L/D = 1$ and $fL/U_{Cavg} = 2.92$ ($N = 3$) for $L/D = 2$. These findings indicate that the peak frequencies of the $Re_D = 12000$ systems with

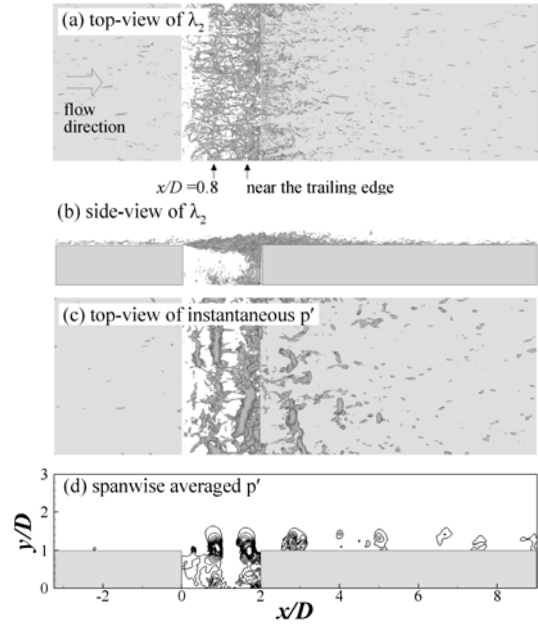


Figure 10: Instantaneous coherent structures; (a) top-view of λ_2 distribution, (b) side-view of λ_2 distribution, (c) top-view of λ_2 distribution, (d) spanwise-averaged p' .

$L/D = 1$ and 2 correspond to the 2nd and 3rd modes ($N = 2$ and 3), just like the oscillating frequency of laminar cavity flows (Gharib & Roshko 1987). Considering that the N th modes of laminar cavity flows are related to the streamwise wavelength (λ_x) of large-scale structures, the observation that the peak frequencies at $Re_D = 12000$ for $L/D = 1$ and 2 correspond to the 2nd and 3rd modes suggests that large-scale vortical structures are present in turbulent cavity flows. Assuming that the streamwise length scale of pressure fluctuations is half of $1/\lambda_x$, the length scale is expected to be $0.4D$ near $x/D = 1.0$ when $L/D = 2$. Note that the streamwise length scale of pressure fluctuations is about $0.45D$ in the laminar case of Chang et al. (2006), for which self-sustained oscillations are observed. The similarity of streamwise length scales supports the existence of large-scale vortical structures in turbulent cavity flows.

Next, to elucidate the large-scale vortical structures responsible for the N th modes, we examined instantaneous flows for the system with a length-to-depth ratio of 2. Figures 10(a) and (b) show a top-view and side-view of the instantaneous coherent structures identified using the λ_2 criterion. Identification using the λ_2 criterion shows only small vortical structures because λ_2 is calculated from the velocity gradient tensor. Nevertheless, the top view of λ_2 (Figure 10(a)) shows a slight clustering of small vortical structures near $x/D = 0.8$ and in the vicinity of the trailing edge. The side view of λ_2 (Figure 10(b)) shows the development of the shear layer, but fails to distinguish the large-scale vortical structures from the shear layer. Compared to the λ_2 criterion, instantaneous pressure fluctuations are better for depicting large-scale vortical structures. As seen in Figure 10(c), quasi two-dimensional vortical structures are observed near $x/D = 0.8$ and in the vicinity of the trailing edge. In the region immediately downstream of the leading edge, another vortical structure is

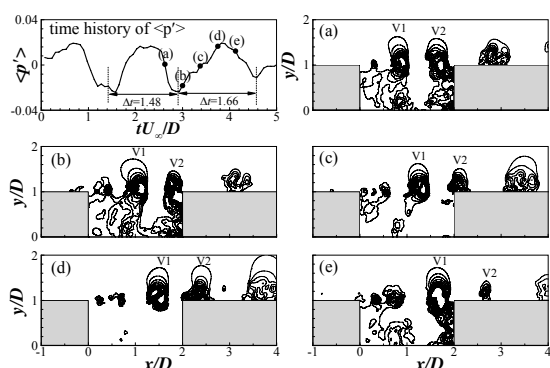


Figure 11: Time history and sequential patterns of spanwise averaged pressure fluctuations. Here $\langle p' \rangle$ represents spanwise averaged pressure fluctuations. Times of (a) ~ (e) are 2.625, 3.0, 3.375, 3.75, 4.125.

likely to be initiated. The large structures are more clearly observed in the contour plot of spanwise-averaged pressure fluctuations shown in Figure 10(d). Figure 11 shows the time history and sequential patterns of the spanwise-averaged pressure fluctuations. The time history records the spanwise-averaged pressure fluctuations measured at $(x/D, y/D) = (1.0, 1.0)$. The pressure fluctuations show quasi-periodic oscillations in the range of $1.4 \leq \Delta t \leq 1.7$, where Δt is the time interval between consecutive large-scale structures. The peak frequency ($\omega_{\text{peak}} = 4.5$) of the energy spectra is in good agreement with the range of the time interval. The sequence of contour plots in Figures 11(a)~(e) show the convective patterns of the large-scale vortical structures.

CONCLUSION

When the turbulent boundary layer approached the leading edge in cavity flows with $Re_D = 600$ and 3000 , the energy spectra of pressure fluctuations showed energetic frequencies in the range of $0.15 \leq \omega_0 \leq 0.3$. Examination of conditionally averaged flow fields revealed that high speed streaky structures in the incoming turbulent boundary layer made the separated shear layer locally unstable and generated the pressure fluctuations with the energetic frequencies. The same energetic frequencies were observed in the flow over a backward-facing step as well as in deep and shallow cavity flows because the high speed streaky structures remained undisturbed in the region immediately downstream of the leading edge. Considering that self-sustained oscillations are meaningful only when the oscillations arise from a geometric peculiarity of the cavity, neither the energetic pressure fluctuations generated by the high speed streaky structures nor the irregular shedding of large-scale vortical structures are regarded as self-sustained oscillations in the incompressible turbulent flow over an open cavity.

In the turbulent cavity flow with $Re_D = 12000$, the peak frequencies of the energy spectra at cavity lengths of $L/D = 1$ and 2 were found to correspond to the N th modes with $N = 2$ and 3 respectively. The observed N th modes were very similar to the frequency characteristics of self-sustained oscillations reported previously for laminar cavity flows.

While the vortex identification revealed a slight clustering of small vortical structures in the vicinity of the large-scale vortical structures, inspection of the instantaneous pressure fluctuations as well as spanwise-averaged pressure fluctuations made it clear that regular shedding of quasi two-dimensional vortical structures was responsible for the peak frequency in the energy spectra. When the large-scale vortical structure impinged on the trailing edge, the structure split into a small part entrained into the cavity along the vertical wall and a large part that was ejected out of the cavity. The characteristics revealed in the present work, particularly the regular shedding and impinging of large-scale vortical structures, strongly suggest that a fully turbulent boundary layer can give rise to self-sustained oscillations in an incompressible turbulent flow over an open cavity.

The authors would like to acknowledge the support from KISTI (Korea Institute of Science and Technology Information) under the 8th Grand Challenge Support Program with Dr. Lee as the technical supporter. The use of the computing system of the Supercomputing Center is also greatly appreciated.

REFERENCES

- Ashcroft, C. & Zhang, X., 2005, "Vortical Structures over Rectangular Cavities at Low Speed", *Physics of Fluids* 17, 015104.
- Chang, K. C., Constantinescu, G. & Park, S. -O., 2006, "Analysis of the Flow and Mass Transfer Processes for the Incompressible Flow past an Open Cavity with a Laminar and a Fully Turbulent Incoming Boundary Layer", *Journal of Fluid Mechanics*. Vol. 561, pp. 113-145.
- Chatellier, L., Laumonier, Y. & Gervais, Y., 2004, "Theoretical and Experimental Investigations of Low Mach Number Turbulent Cavity Flows", *Experiments in Fluids* Vol. 36, pp. 728-740.
- Gharib, M. & Roshko, A., 1987, "The Effect of Flow Oscillations on Cavity Drag", *Journal of Fluid Mechanics*, Vol. 177, pp. 501-530.
- Grace, S. M., Dewar, W. G. & Wroblewski, D. E., 2004, "Experimental Investigation of the Flow Characteristics within a Shallow Wall Cavity for both Laminar and Turbulent Upstream Boundary Layers", *Experiments in Fluids*, Vol. 36, pp. 791-804.
- Lin, J. -C. & Rockwell, D., 2001, "Organized Oscillations of Initially Turbulent Flow past a Cavity", *AIAA J.*, Vol. 39 (6), pp. 1139-1151.
- Norton, D. A., 1952, "Investigation of B47 Bomb Bay Buffet", Boeing Airplane Co. Document No. D12675.
- Pereira, J. C. F. & Sousa, J. M. M., 1994, "Influence of Impingement Edge Geometry on Cavity Flow Oscillations", *AIAA J.*, Vol. 32, pp. 1737-1740.
- Pereira, J. C. F. & Sousa, J. M. M., 1995, "Experimental and Numerical Investigation of Flow Oscillations in a Rectangular Cavity", *Journal of Fluids Engineering*, Vol. 117, pp. 68-74.
- Rockwell, D., 1998, "Vortex-Body Interactions", *Annual Review of Fluid Mechanics*, Vol. 30, pp. 199-229.